

## **Review Essay**

**Towards Surface Plasmon Polaritons on Flexible Substrates.**

**Pierre Eugene Valassakis  
Student ID: 100004548  
Supervisor: Dr. Andrea Di Falco  
Level: BSc**

**6370 words**

## Towards Surface Plasmon Polaritons on Flexible Substrates.

### **Abstract**

Scientific interest in the field of plasmonics has been accompanied with a tremendous development of flexible electronics. It is now conceivable to have controlled surface electromagnetic waves in fully integrated flexible circuits with a significant impact in various areas from material science to biology, chemistry or environmental science. In this article the fundamentals of the field of plasmonics and the recent advances in nanotechnologies, metamaterials and flexible electronics that are relevant towards the realisation of this ideal are presented.

### **I. Introduction**

Plasmonics is the field of research that deals with confined electromagnetic (EM) fields at the surfaces of metal-dielectric boundaries. As it is visible from Fig.1, interest in the field has been drastically increasing since the 50's [1].

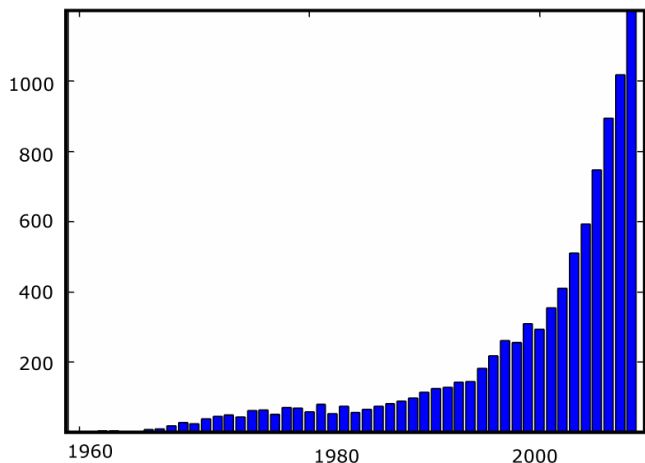


*Figure 1: Number of papers containing "surface plasmon" in their title as a function of the year.  
Taken from [1].*

This increasing interest is not only sparked by fundamental science and the investigation of subwavelength optics [2-4], but also comes from the exciting potential applications of plasmonic devices [3-7]. In fact, these bridge the gap between conventional photonic and electronic systems and have the potential to lead to fully integrated photo-electronic devices [6-8]. Concrete applications can be found in solar cells [3,5], Surface-Enhanced Raman Spectroscopy (SERS) [2,3,40], chemical sensors [2,3,10], data storage and information transfer in integrated circuits [3,8]. Also, recent advances in flexible electronics [11-21], metamaterials [9, 22-24] and nanofabrication in flexible substrates [22,25] have opened new paths to applications such as biocompatible electronics [17,19,18] and biosensors [3,7,10]. It is therefore now conceivable and relevant to have broadband and flexible plasmonic coupling devices, with applications in photo-

electronic and biocompatible circuits that operate in the visible range [6,22,24, 61,62]. Defining parameters of such couplers are the wavelength of operation along with the working angles of incidence, the efficiency of coupling, the spatial extent and miniaturisation potential of the system, and the flexibility properties of the structure [3,26,37,38]. Other desirable properties of such schemes would be cost efficiency, ease of operation and mass production compatibility for industry-based applications.

This review will then focus on the information relevant towards the realisation of a coupling scheme displaying high efficiencies over a large range of frequencies in the visible spectrum regardless of the angle of incidence, and that can display flexibility properties to be compatible with flexible electronics. In particular, basic theory behind Surface Plasmon Polaritons (SPPs), the most common and noteworthy techniques for exciting them as well as recent advances on flexible nanostructures and electronics are reviewed.

## **II. History**

Plasmonics, Surface Plasmon Polaritons and their relations to metallic nanostructures had already found applications in everyday experience before anything was known about

their existence. At the time, gold nanoparticles of different sizes imbedded in glasswork resulted in bright colours being emitted [1,26-28]. The most famous example, dating back to 4<sup>th</sup> century AD, is Lycurgus Cup [1,26,28], which appears green when lightened from outside but turns bright red when illuminated from within as illustrated in Fig.2 below:



*Figure 2: Pictures of Lycurgus Cup. Illuminated from within (right), it is bright red while under normal lighting (left) it appears green. Taken from [1].*

The first occurrence of SPPs in a scientific research context is attributed to Prof. R. W. Wood in 1902 with his discovery of an “unusual” intensity distribution of the reflection pattern when p polarised light is shone onto a metallic grating [3,5,29,30]. At the same time, in 1904, Maxwell Garnet performed studies on the effects of doping glass with metals [1,3]. It was only in 1908 that a more complete theoretical approach

was used in Mie's description of light scattering from spherical particles, even though the description was not yet interpreted in terms of surface plasmons [1,3,26]. The next milestones in the subject were achieved in the 50's with the theoretical and experimental investigation of energy losses of fast electrons fired on metal films [1,3,27]. Pines and Bohm theoretically described such phenomena by considering collective oscillations of electrons in metals which were called "plasmons" [1,3,27]. In 1957, Ritchie completes the picture by considering boundary effects in such experiments, hence predicting the existence of surface plasma oscillations [1,3,27]. The existence of such surface electron excitations was confirmed shortly after in experiments performed by Powell and Swan, and the name "surface plasmon" was used for the first time by Stern and Ferrell to describe their quantum [1,27,31]. Subsequently, Ritchie also used this theory to explain the intensity patterns obtained using a metallic diffraction grating, therefore explaining Wood's "anomalies" [3,32]. Other theoretical studies of the subject followed with for instance McPhedran and Maystre's work in 1974 [33]. The next step towards modern understanding was achieved by Kretschmann and Otto in 1968 [1,3,27,34,35]. In their works, they demonstrated excitation of SPPs using photons instead of electron impact, and

overcame the momentum mismatch by having the incoming photons incident through a prism [35,36,37]. In more recent years, the emergence of nanotechnologies and new techniques such as electron beam lithography [38, 39], spin-coating [42,43], beam milling [26,41], lift-off [38], stencil lithography [22], nanoimprinting [25], metamaterials [9, 22-24] and direct near-field microscopy [4] have driven research and opened many new application prospects.

### III. Theory of Surface Plasmon Polaritons.

The underlying physics of SPPs is understood using a classical framework and applying Maxwell's equations in a metal-dielectric boundary. This is done thoroughly in Maier's *Plasmonics : Fundamentals and Applications* [37], and the key points are summarised here. Jackson's *Classical Electrodynamics* [44] is also a good starting point to the unfamiliar reader. The reason for not requiring recourse to quantum mechanics in treating the subject is the closely spaced electron energy levels within most metals, with typical energy spacings negligible compared to the thermal excitation energy at reasonable temperatures [37]. The possibility of interband transitions that can occur in real metals for sufficiently high photon energies is also ignored [37].

As a first step, it is important to look at some properties of electromagnetic fields in media,

which here are assumed to be isotropic, linear and nonmagnetic. In this case, Maxwell's equations have the following form [37]:

$$\nabla \cdot \mathbf{D} = \rho_{ext} \quad (1)$$

$$\nabla \times \mathbf{E} = -\frac{\partial \mathbf{B}}{\partial t} \quad (2)$$

$$\nabla \cdot \mathbf{B} = 0 \quad (3)$$

$$\nabla \times \mathbf{H} = \mathbf{J}_{ext} + \frac{\partial \mathbf{D}}{\partial t} \quad (4)$$

with

$$\mathbf{D} = \epsilon_0 \epsilon \mathbf{E} \quad (5)$$

$$\mathbf{H} = \mu_0 \mu \mathbf{B} \quad (6)$$

In the above,  $\mathbf{D}$  is the electric displacement;  $\mathbf{H}$  is the auxiliary field,  $\mathbf{B}$  the magnetic field and  $\mathbf{E}$  the electric field.  $\rho_{ext}$  and  $J_{ext}$  represent the external current and charge density, as defined in Maier [37] and also in Marder's *Condensed Matter Physics* [45].  $\epsilon_0$  and  $\mu_0$  are the permittivity and permeability of free space,  $\mu = 1$  is the relative permeability of a non-magnetic medium and  $\epsilon$  is the complex valued dielectric constant determining the optical and dispersive properties of the medium. It relates to its complex refractive index by  $n' = n(\omega) + i\kappa(\omega) = \sqrt{\epsilon}$  [37], and for transverse waves determines the dispersion relation  $k^2 = \epsilon(\mathbf{k}, \omega) \frac{\omega^2}{c^2}$  [37]. It is also noticeable that  $\kappa(\omega) = \frac{Im(\epsilon)}{2n(\omega)}$  is related to Beer's law, which gives the decrease in the intensity of the radiation through a medium

as  $I(x) = I_0 e^{-ax}$  where  $a = \frac{2\kappa\omega}{c}$  [37]. For metals, by considering the plasma model where carriers consist of a free electron gas, it is possible to show that the dielectric constant takes the form  $\epsilon = \epsilon' + i\epsilon''$ , where [37]:

$$\epsilon' = 1 - \frac{\omega_p^2 \tau^2}{1 + \omega^2 \tau^2} \quad (7)$$

$$\epsilon'' = \frac{\omega_p^2 \tau}{\omega(1 + \omega^2 \tau^2)} \quad (8)$$

In equations (7) and (8),  $\tau$  represents the relaxation time of the free electron gas and  $\omega_p$ , called the plasma frequency, is the characteristic frequency of bulk oscillations of electrons against the positive ions of the lattice. It is important to consider the implications of different frequency regimes. At low frequencies  $\omega \ll \omega_p$ ,  $\epsilon''$  is significant, and using Beer's law the metal becomes closer and closer to a perfect conductor. For  $\omega \lesssim \omega_p$ ,  $\omega\tau \gg 1$  and  $\epsilon$  is mostly real with  $\epsilon(\omega) \approx 1 - \frac{\omega_p^2}{\omega^2}$ . Finally for frequencies  $\omega > \omega_p$ , the material loses its metallic character and becomes transparent to radiation with dispersion  $\omega(k)^2 = \frac{\kappa^2 c^2}{\epsilon} = \omega_p^2 + k^2/c^2$ . Here, it is only relevant to consider the case  $\omega < \omega_p$  [37].

Surface Plasmon Polaritons are electromagnetic excitations confined at a metal-dielectric interface. The electromagnetic oscillations are coupled to

electron oscillations within the metal, which is why they are called polaritons [3]. We can define the system configuration as appears in Fig.3 below:

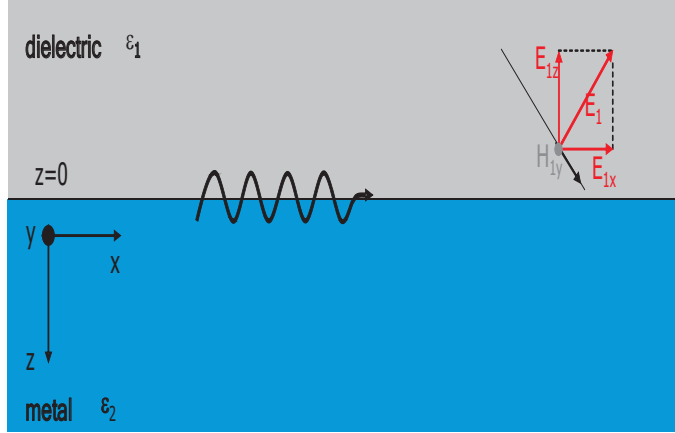


*Figure 3: Geometry of the system. Consists of a slab of complex dielectric constant  $\epsilon_2$  for  $z < 0$  and a dielectric medium of real and positive dielectric constant  $\epsilon_1$  for  $z > 0$ .  $\epsilon_2$  is assumed only to depend on  $z$  for simplicity. Taken from [26].*

Using Maxwell's equations, one can then get to the usual wave equation [37]:

$$\nabla^2 \mathbf{E} - \frac{\epsilon}{c^2} \frac{\partial^2 \mathbf{E}}{\partial t^2} = 0 \quad (9)$$

applicable to both media. Solving (9) in this case for a wave propagating in the  $x$  direction yields two sets of solutions called s and p modes [3,26,37]. The former consist of an electric field in the  $y$  direction and a magnetic field in the  $x$  and  $z$  direction. P modes, also

called ansatz or transverse magnetic (TM) modes [26], consist of a magnetic field in the  $y$  direction and an electric field in the  $x$  and  $z$  directions. As it is shown in Maier [37], applying boundary conditions for s modes leads to a trivial solution. It is therefore only relevant to focus on p modes, which have the following form [3]:

$$\mathbf{E}_1 = (E_{x1}, 0, E_{z1}) \exp(-k_{z1}z) \exp[i(k_x x - \omega t)] \quad (10)$$

$$\mathbf{H}_1 = (0, H_{y1}, 0) \exp(-k_{z1}z) \exp[i(k_x x - \omega t)] \quad (11)$$

for  $z > 0$  and

$$\mathbf{E}_2 = (E_{x2}, 0, E_{z2}) \exp(-k_{z2}z) \exp[i(k_x x - \omega t)] \quad (12)$$

$$\mathbf{H}_2 = (0, H_{y2}, 0) \exp(k_{z2}z) \exp[i(k_x x - \omega t)] \quad (13)$$

for  $z < 0$ .

Further applying continuity conditions at the surface and requiring  $\mathbf{H}$  to satisfy the wave equation yields [3,37]:

$$\frac{k_{z2}}{k_{z1}} = -\frac{\epsilon_2}{\epsilon_1} \quad (14)$$

$$k_{z1}^2 = k_x^2 - k_0^2 \epsilon_1 \quad (15)$$

$$k_{z2}^2 = k_x^2 - k_0^2 \epsilon_2 \quad (16)$$

Rearranging this gives the dispersion relation for SPPs which is the key relation in their study:

$$k_x = k_0 \sqrt{\frac{\epsilon_1 \epsilon_2}{\epsilon_1 + \epsilon_2}} \quad (17)$$

Where  $k_0 = \frac{\omega}{c}$  is the wavenumber of the EM wave in vacuum [3,37].

Before discussing the implications of eq.17 it is relevant to consider those following from the previous equations. As it is visible from eq. (10)-(13), in order to get SPPs, the wavenumbers  $k_{z1}$  and  $k_{z2}$  need to be real and positive. This leads the fields to exponentially decay with increasing  $|z|$ , which gives confinement at the surface as required. From this and eq.14,  $\epsilon_2$  and  $\epsilon_1$  need to be of opposite sign, confirming that SPPs exist at a metal-dielectric boundary. Also, one can define the skin depths  $\delta_d = 1/|k_{z1}|$  and  $\delta_m = 1/|k_{z2}|$  in the dielectric and the metal which are the distances in z over which the electric field is reduced by e [3]. Using (15), (16) and (17), those can be expressed as [3]:

$$\delta_d = \frac{1}{k_0} \left| \frac{\epsilon_1 + \epsilon_2}{-\epsilon_1^2} \right|^{1/2} \quad (18)$$

$$\delta_m = \frac{1}{k_0} \left| \frac{\epsilon_1 + \epsilon_2}{-\epsilon_2^2} \right|^{1/2} \quad (19)$$

In general, the skin depth is larger for the dielectric than for the metal. This is illustrated in Fig.4 below, which also gives an intuitive representation of SPPs:

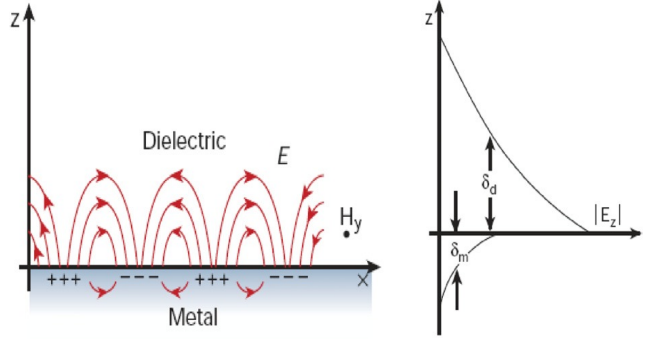


*Figure 4: Illustration of SPPs: Electric field and electron oscillations at the metal-dielectric boundary (right) and evanescent decay of the electric field with increasing  $|z|$  (left). Taken from [3].*

It is important to note that in the treatment so far it was implicitly assumed that the metal's dielectric constant is approximately real, hence that the regime of operation is for  $\omega$  close to  $\omega_p$ . When considering the imaginary part of  $\epsilon_2$ , one finds that  $k_x$  has an imaginary component, which leads to an extra damping term  $\exp(-Im(k_x)x)$  in the field expressions due to ohmic dissipation with the electron oscillations. This also leads to a characteristic propagation length  $\delta_{SP} = \frac{1}{2Im(k_x)}$ , which is of the order of  $10^{-6} - 10^{-4} m$  [26,37]. It is also essential to be aware that the treatment is only valid in the approximation of a thick metallic slab. For a thin metal film within a dielectric, SPPs on the top and the bottom of the film can interact, leading to a different dispersion and the appearance of a symmetric and an antisymmetric branch [37]. The

symmetric SPP mode also has a much larger propagation length that can even be of the order of centimetres, which leads to the so-called LRSPPs (long-range SPPs) [3,37].

Back to eq.17, it is possible to plot the dispersion relation of the SPPs in a typical metal/ dielectric interface as well as the dispersion relation of the EM radiation within the dielectric, the “light line” [37]. Such a plot appears in Fig.5 below:

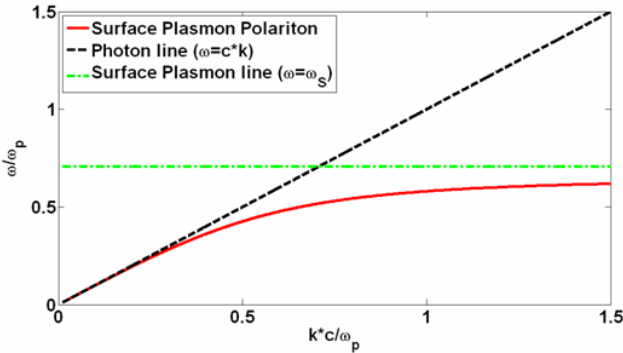


*Figure 5: Illustration of the dispersion relation of SPPs and of the light line in the dielectric, normalised with the plasma frequency  $\omega_p$ . Taken from [46].*

Within the dielectric, the dispersion relation is  $\omega = \frac{c}{\sqrt{\epsilon_1}} k$  [3, 26, 37, 47]. Comparing this with eq.17, one realises that the SPP dispersion relation always lies to the right of the light line as it also appears in Fig.5. This implies that incident photons within the dielectric cannot excite SPPs directly, as energy and momentum cannot be simultaneously conserved: for a given  $\omega$ ,

$k_{xphoton} < k_{xSPP}$  [26,37]. Moreover, the situation is worsened in a realistic setup, where the photons are incident at some angle, as the x-component of the photon wavevector will further decrease. Hence, to be able to excite SPPs light there needs to be some extra momentum provided to the incident photons. Finding ways to do so in increasingly more efficient and less restrictive manner is still a matter of research.

#### **IV. SPP coupling techniques**

##### **A. Prism coupling**

Kretschmann and Otto (1968) [34,35] overcame the momentum mismatch by using total internal reflection on a prism, in the configurations shown in Fig.6 below:

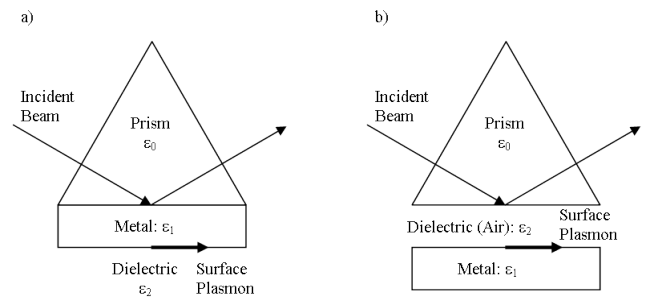


*Figure 6: Kretschmann (left) and Otto (right) configurations. Taken from [48].*

In both cases, a prism with dielectric constant  $\epsilon_p$  is used near a thin metallic film with

dielectric constant  $\varepsilon_1$ , in order to excite SPPs in the interface between this metal and a second dielectric with dielectric constant  $\varepsilon_2$ . Within the prism, the dispersion of light reads  $\omega = \frac{c}{\sqrt{\varepsilon_p}} k$ . Hence, for a given frequency  $\omega$ , the x-component of the wavevector of the incident beam is  $k_x = k_0 \sqrt{\varepsilon_p} \sin(\theta)$  [37] where  $k_0$  is the wavenumber in vacuum and  $\theta$  is the angle of incidence. As  $\varepsilon_p > \varepsilon_2$ , it is possible to have  $k_{x\text{photon}} = k_{x\text{SPP}}$  for the right angle of incidence, in which case an SPP can be excited on the metal-dielectric interface. Excitation happens upon reflection of the incident beam on the surface of the prism and through tunnelling of the photons through the metal slab/dielectric layer (depending on whether the Kretschmann or Otto configurations are used, respectively) [37]. Successful excitation of SPPs is then manifested by a dip in the intensity of the reflected beam from the prism, and for that reason this coupling scheme is also called attenuated total internal reflection [3,26,34,35,37]. It can be noted that the Otto configuration is somewhat less restrictive, as the prism does not need to be in direct contact with the slab and hence can be used in systems not specifically configured for that purpose [37].

Even though these techniques have been an important stepping-stone in the field, it is important to note many strong limitations

associated with them. Specifically, for a given frequency, only photons incident at a specific angle will be coupled to SPPs and conversely for a given angle of incidence only photons with a specific frequency will be coupled. Also, these configurations require a macroscopic, restrictive setup, which is less than ideal for integrating into a practical system. Subsequently, many theoretical and experimental investigations have taken place using different prism configurations and achieving various specific goals, they remain however mainly impractical [49-55].

As an interesting highlight, John O'Hara et al. have demonstrated broadband coupling to SPPs in the THz regime using prisms, however the setup remains quite cumbersome and does not rely on attenuated total internal reflection [50]. Another noticeable paper comes from Tetsuo Kan et al. [51], which achieved miniaturisation of a Kretschmann-like configuration with a repeated array of Silicon nanoprisms as shown in Fig.7 below:

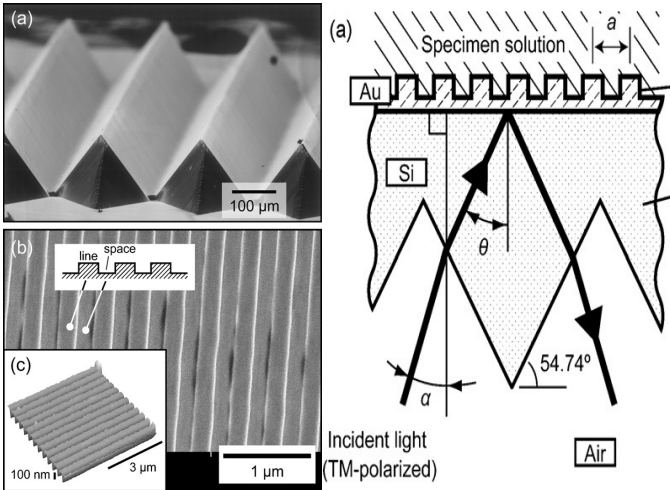


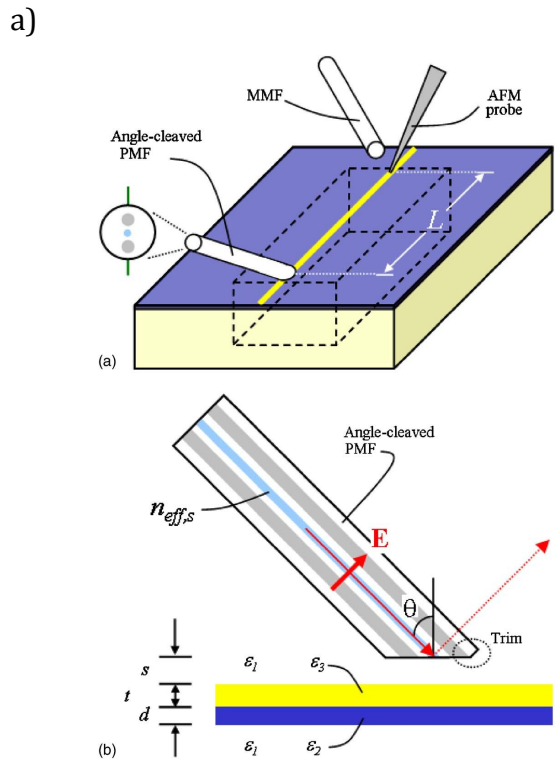
*Figure 7: Configuration used by Tetsuo Kan et al. with a grating placed on top of Silicon nanoprisms. Right: Cross sectional illustration of the device. Left: Scanning Electron Microscope (SEM) and Atomic Force Microscope (AFM) images of the device. Taken from [51].*

The prisms are micrometre scale (Fig.7), which demonstrates the possibility of miniaturisation of such devices in order to enhance their applicability. However, such a configuration is still quite rigid and subject to limitations, with the above setup only functioning in the near infrared for instance, as silicon is only transparent in this regime. Also, a grating had to be used on top of the prism to achieve the momentum match, because at the available angles of incidence the prisms alone weren't enough [51]. Few other publications are concerned with nanoprism fabrication, they do not however involve organised arrays that would be

necessary to surface plasmon excitation [53,56-58]. To date, no configuration has been found using prisms that truly achieves broadband coupling with a potential of integration to practical systems.

### B. Excitation through an angle-cleaved optical fiber.

Over the years, many other methods for SPP coupling have been found. Robert Charbonneau et al. [59] have demonstrated a method involving a polarisation-maintaining optical fiber (PMF). The optical fiber is angle-cleaved in one facet and allows very efficient coupling in a way similar to prism coupling. Charbonneau's setup and results are presented in Fig.8 below:



b)

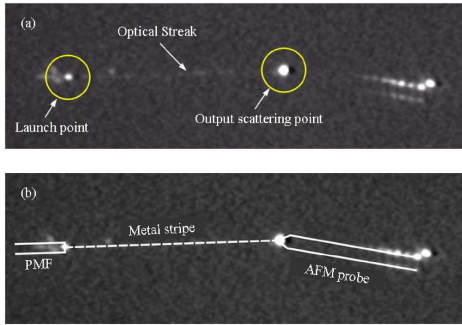


*Figure 8: Angle-cleaved PMF excitation method.* a) *Setup schematic, SPPs are excited at the PMF end and then travel though a metal stripe to the decoupling end composed of an atomic force microscopy probe that generates an optical signal from the SPPs and a multimode fiber (MMF) that collects this signal (top). A cross section of the excitation end is also shown in more detail (bottom), with the electric field perpendicularly polarised with respect to the direction of the fiber.*  
 b) *Microscope image of the setup at work (top), annotations for the location of the different parts of the setup (bottom). Taken from [59]*

This method has the advantage of being simpler to align in the sense that there is only the PMF angle to adjust [59]. However, once the setup is complete, it has the restrictive requirement that the angle of incidence has to remain fixed [59].

### C. Near-field excitation: a localised excitation scheme

Another important coupling scheme has been introduced by Hecht et al. [60]. In their work, they have demonstrated a way to excite SPPs at a very precise location that acts as a point-like source of surface plasmons. To achieve this, the tip of a near-field microscope has been used for coupling [60]. Although the setup used by Hecht is relatively complex, the principle is quite simple, and is illustrated in Fig.9 below [37]:

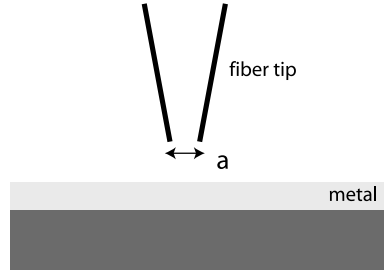


*Figure 9: Illustration of the working principle of a near-field excitation setup. Taken from [37].*

The method relies on the fact that the tip illuminating the metal has subwavelength aperture size  $a \lesssim \lambda_{SPP} \lesssim \lambda_{incident}$  (Fig.9) [37]. With such a small aperture tip compared to the wavelength, the transmitted radiation will have wavevectors that are bigger than those of free photons in the medium, which is visible by considering its Fourier transform [60]. This way, phase matching can be achieved at the tip, and therefore local SPP

excitation accomplished [37].

#### D. Excitation via highly focused white-light continuum

For broadband coupling, Bouhelier and Wiederrecht [61] have presented a completely different setup [61,37]. Using a lens configuration, a broad continuum of wavelengths is used in order to excite SPPs. This setting is illustrated in Fig.10 below:

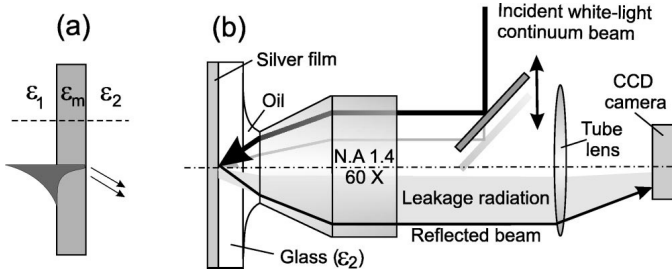


*Figure 10: Broadband coupling setup using a focused continuum beam. The apparatus uses an oil-immersion objective (right) in order to excite SPPs in a silver film (left). Leakage radiation is then collected by the same objective and visualised using a CCD camera. Taken from [61].*

The incident white light is highly focused using an objective with a high numerical aperture, which results in a wide angular spread of the radiation incident on the glass and silver film [37,61]. This angular spread is at the origin of the broadband coupling, as for each frequency there is some angle available

where momentum matching can be achieved in a way similar to prism coupling [37]. As they travel through the metal film, and due to its increasing thickness, the surface plasmons decouple producing far field free photons [61]. The broadband SPPs excited this way on the silver film can be subsequently detected by the same objective through this leakage radiation that they generate, as it is illustrated in Fig. 10 [37,61]. Using this method, Bouhelier and Wiederrecht studied the effect of the frequency used on the propagation length of the SPPs [61]. The results obtained are shown in Fig.11 below:

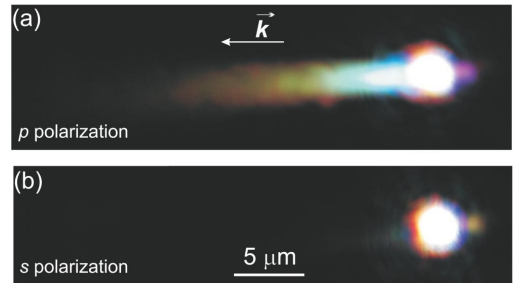


*Figure 11: Detection of leakage radiation from the objective. Results for p polarised (top) and s polarised (bottom) light. Taken from [61].*

As s polarised light cannot excite SPPs, such an incident beam is used for comparison [61]. It is then clearly visible from Fig.11 that for p polarised light only, SPPs of different frequencies have been excited and propagate through the silver film [61]. Different frequencies propagate though different distances which produces the colour

decomposition of the leakage radiation (Fig.11) [61].

This work is quite impressive in that it truly achieves broadband coupling, it relies however on a spatially extended system and efforts for miniaturisation need to be made for its integration in practical configurations.

### E. Plasmonic waveguide coupling: towards integration in electronic circuits.

Such efforts to find SPP coupling schemes that can be integrated to electronic systems have been seen, as for instance in the system proposed by Jie Tian et al. [62]. In this paper, a plasmonic waveguide was inserted between two silicon waveguides and a coupling efficiency of up to 35% was demonstrated [62]. The setup is illustrated in Fig.12:

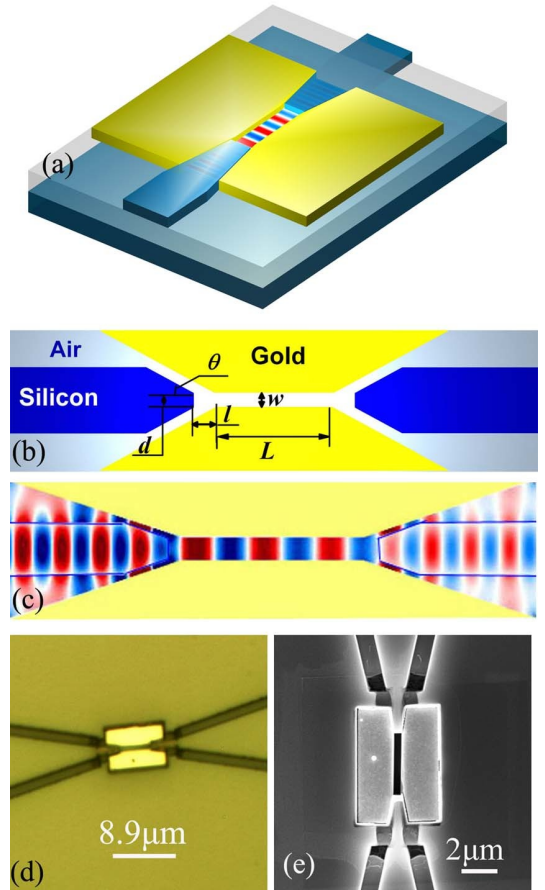


Figure 12: a) Broad view of the system configuration. b) Schematic of the waveguides with the system parameters: the plasmonic wave guide is located between two silicon waveguides and is composed of a gap of width  $w$  in between two gold plates. c) Field distribution simulation at  $1.5\mu\text{m}$  using the three dimensional finite-difference time domain method. d) optical microscope and e) SEM images of the system. Taken from [62].

As it is also shown in the pictures in Fig.12 d) and e), this system is remarkable in that it achieves SPP coupling and is of micrometre dimensions. This demonstrates the possibility

of integrating plasmonic devices within electronic systems. The configuration also achieves broadband coupling, which is another advantage [62]. The physics behind this arrangement was theoretically investigated by Dal Negro, Feng, and Brongersma [76, 77]. In short, it relies on the fact that the subwavelength width  $w$  (see Fig.12 b)) of the plasmonic waveguide allows for the associated dispersion relation to be above the silicon light line [76,77].

In the same spirit of creating plasmonic systems compatible with modern electronics, one can also note Stegeman's et al. [63] work on end-firing coupling [37,63]. In this scheme, coupling is achieved by matching the spatial field distribution of a waveguide [37]. Efficiencies up to 90% have been demonstrated [37,63], but this method is limited by the possible system geometries where high efficiency coupling can be achieved [37].

## **F. The grating-coupling scheme**

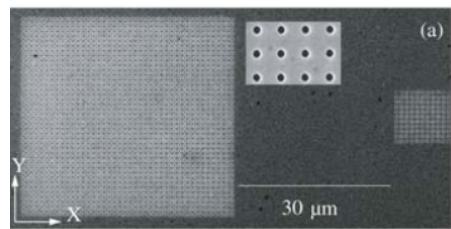
A final very common method for exciting SPPs consists on the use of gratings or hole arrays in the metallic surface in order to provide the extra momentum needed. If a grating with lattice constant  $a$  is used then the condition for successful excitation of SPPs becomes [37]:

$$k_{xSPP} = k_{photon} \sin(\theta) + \frac{2\pi}{a} n \quad (20)$$

where  $k_{photon} \sin(\theta)$  is the x component of the wavevector of the incident photon in the dielectric,  $\frac{2\pi}{a}$  is a reciprocal lattice vector and  $n$  is an integer [37]. Because of the second term in eq.20 it is then again possible to match the wavenumbers for a given frequency and generate surface plasmons.

Gratings and their relation to SPPs have been thoroughly investigated during the years [29,30,32,64-71]. One noticeable paper comes from Deveaux et al. [71], which demonstrates quite clearly how gratings can be used to couple and decouple surface plasmons [37,71]. Fig.13 below shows the grating setup and a near field-optical image of the SPP coupling and decoupling.

a)



b)

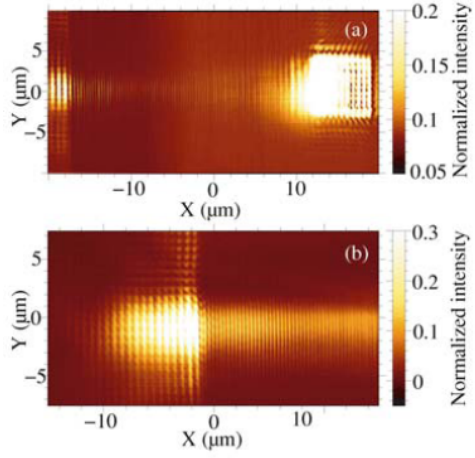


*Figure 13: a) SEM image of the arrangement of holes with period 760nm and hole diameter of 250 nm. b) Near-Field Optical image of the coupling and decoupling of SPPs. Taken from [71].*

By focusing a Ti-sapphire laser at normal incidence on the smaller array (on the right in Fig.13 a)), SPPs were excited, travelling to the array on left where they decoupled into free photons (easily detected as the far field intensity increased) [37,71]. This work demonstrates the feasibility of using SPPs in a controlled manner, which can then be used in photonic circuits for instance [71].

Such efforts in controlling the propagation and behaviour of SPPs, in the perspective of using them in practical applications, are generally visible. Ropers et al. [70] for instance have used SPPs, excited via a grating and propagating towards a conical tip, in order to create a point-like light source. This is illustrated in Fig.14 below:

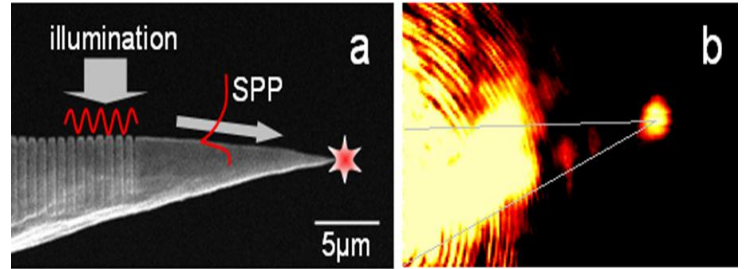


*Figure 14: a) Scanning electron microscope image of the conical tip with the coupling grating and superimposed illustration of the procedure. b) Microscope image of the far field when the device is illuminated. Taken from [70].*

In the above, light of the appropriate wavelength is shone onto the coupling grating, which then excites SPPs travelling towards the conical tip. At the apex, SPPs decouple into light again, creating a point-like light source at the tip of the cone [70].

An important issue to note however is that all these grating methods are mostly limited by the discrete number of available wavevectors that can be provided by the grating surface, therefore not allowing for flexibility in the range of working frequencies. They also widely rely on the use of rigid substrates, which wouldn't allow their use in flexible and deformable systems.

## V. Metamaterials: the current trend towards flexible plasmonic devices.

### A. Broadband coupling

Progress in addressing some of the issues has been made in recent years, especially with the development of metamaterials [9,22-24].

Towards broadband coupling, Shulin Sun et al. [23] have demonstrated a much less restrictive configuration. Using a gradually shrinking “H” pattern, they carefully engineered the permittivity and permeability properties of the tested surface [23]. This way they obtained a range of available momentum increases for incident light to be able to couple to SPPs at the given frequency. Using such a configuration, the incident wavevector does not need to match an exact value but only needs to be smaller than some characteristic value  $\xi$  [23]. Hence, they have shown very efficient coupling for any angle of incidence bigger than a certain critical angle. Conversely, this could have been applied for a given angle of incidence and for a range of incident wavevectors, i.e. broadband coupling. These results are quite significant, even though broadband coupling is still limited by the value of the parameter  $\xi$  and/or the critical angle of incidence [23]. This also still relies on rigid, conventional substrates and has not been tested on bended surfaces [23].

### B. Metamaterials in flexible substrates.

It is however important to note that efforts are being made towards this direction. Nanofabrication techniques that are compatible with flexible surfaces have started to appear [22, 25,72]. These generally rely on an elastomer, usually PDMS (poly(dimethylsiloxane)), to act as a mould or as a substrate in order to create the desired patterns [12,22,72]. Serap Asku et al. [22], in their recent publication, have used nanostencil lithography (NSL) as a more direct nanofabrication technique. As illustrated in Fig.15, this technique relies on the application of a patterned stencil on a flexible substrate. Deposition of the desired material is then performed before removing the stencil, leaving the material at the pattern positions on the substrate [22].

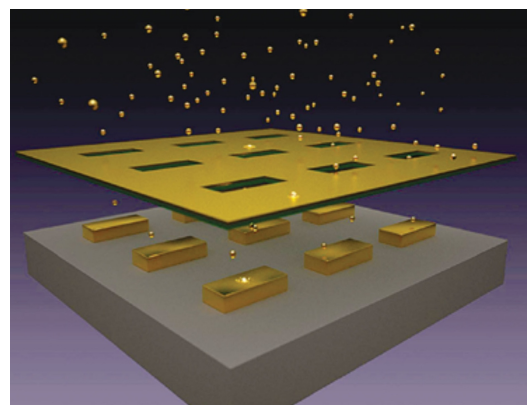
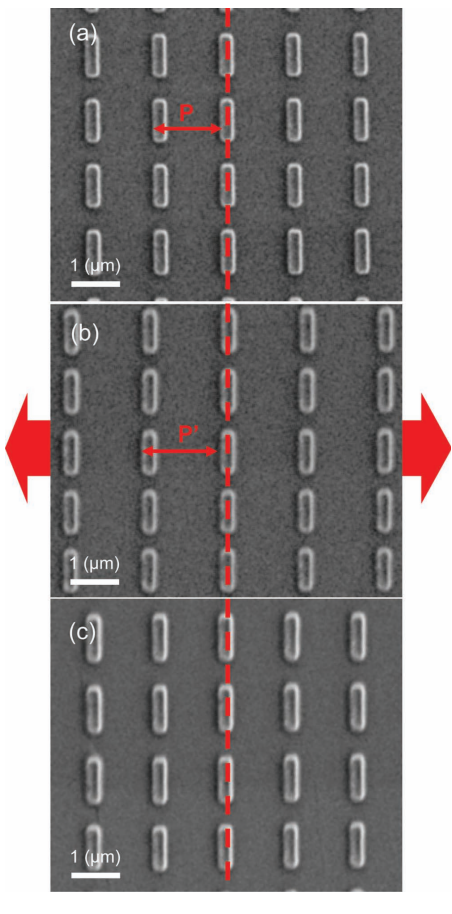
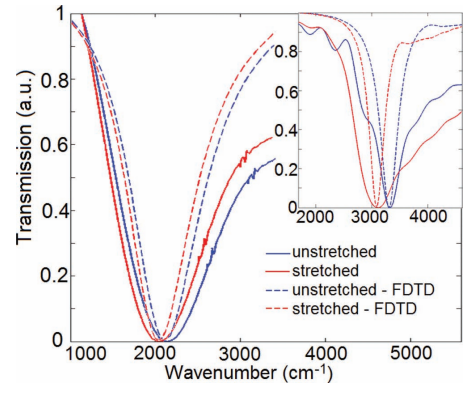


*Figure 15: Schematic of the nanostencil lithography technique. Taken from [73].*

Using NSL, Aksu et al. fabricated microscopic bow-tie structures and plasmonic nanoantennas, which they subsequently optically characterised using infrared light. They also investigated the effect of stretching the flexible PDMS substrate of the nanoantennas by applying a mechanical force. It was observed that the antennas were undamaged by the stretching, but as the periodicity constant of the array increased, the characteristic intensity dip of the spectrum got red-shifted [22]. These results appear in Fig.16 below:



A)



B)

*Figure 16: A) SEM images of the nanoantenna array (a) The array with lattice constant  $P$  (b) Mechanical stretching is applied, resulting in the array having a bigger lattice constant  $P'$ . (c) After the tension was released, the antennas were undamaged. B) Experimental (solid lines) and numerical (dashed lines) transmission spectra. When the PDMS was stretched, a 160 nm redshift was observed. Taken from [22].*

One can note that this is consistent with the simple picture in eq.20: if the constant  $a$  increases  $k_{\text{photon}}$  needs to decrease, or equivalently the wavelength needs to increase, in order to keep  $k_{x\text{SPP}}$  constant at a given frequency. These results are quite significant as they represent a first step towards flexible and stretchable plasmonics. More recently, work performed by Di Falco et al. [24] has demonstrated the fabrication of metamaterials on flexible substrates that can support surface plasmons over visible wavelengths. The approach adopted here is

quite different, with the membrane assembled in a layer-by-layer manner as shown in Fig.17 [24]:

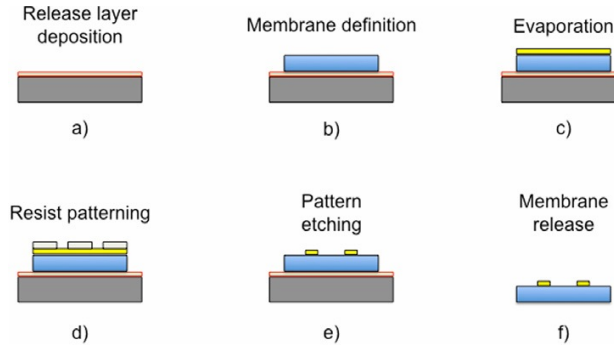


*Figure 17: Fabrication process schematics for the flexible plasmonic membrane. Taken from [24].*

The optical characterisation has been completed using a white light source [24] and the transmission curves and a SEM image of the membrane surface appear in Fig.18 below:

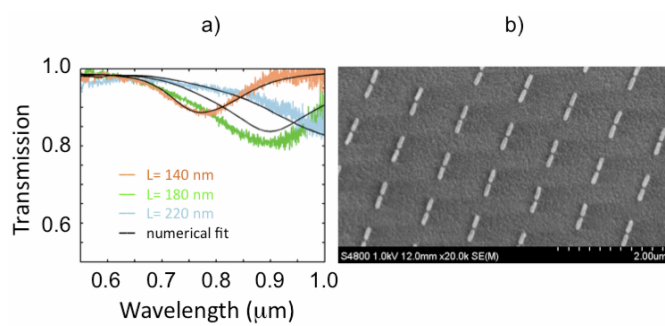


*Figure 18: Transmission curves at different wavelengths (Left) and SEM picture of the membrane surface (right). Taken from [24].*

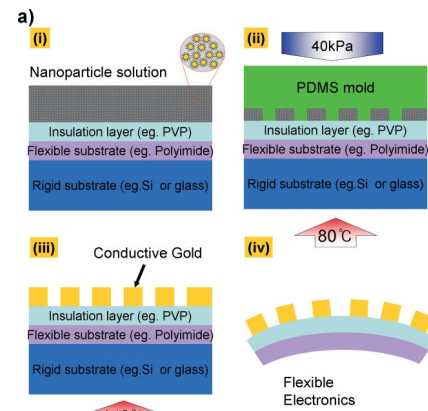
The curves in Fig.18 show the characteristic

dip in intensity demonstrating plasmonic resonances at the given wavelengths [24]. This work does not present however the effects of bending or stretching the fabricated membrane [24].

### C. An interesting Nanofabrication technique compatible with elastic substrates.

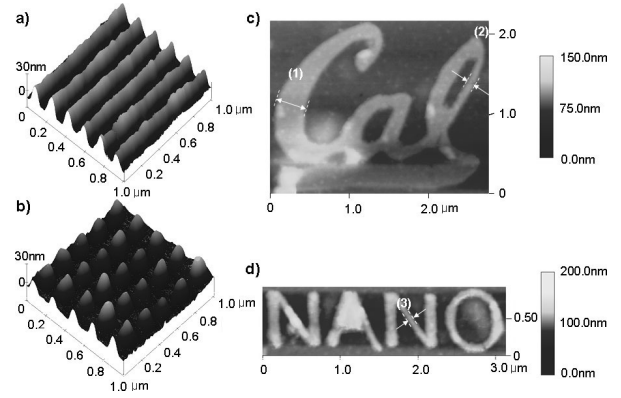
As it is clearly visible from the above, all these advances would not have been possible without the parallel development of nanotechnologies and methods to create microstructures in both flexible and rigid substrates. It is therefore relevant to mention and present a recent paper produced by Inkyu Park et al. [25], which proposed an elegant method for creating nanostructures on flexible materials.

In this letter, a methodology for direct nanoimprinting of metal nanoparticles onto flexible substrates has been presented [25]. The method is illustrated in Fig.19 below:



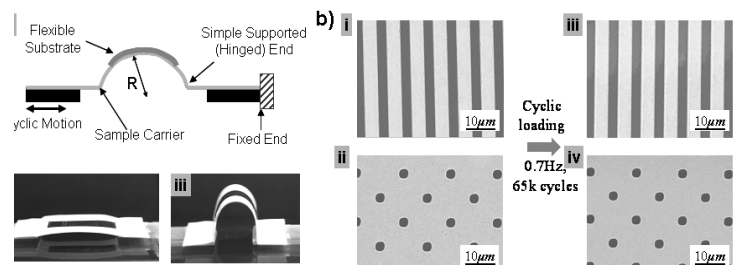
*Figure 19: Park's direct nanoimprinting method illustration. Taken from [25].*

This method does not require extreme temperature and pressure conditions, which is why it is compatible with flexible substrates [25]. The key to this process relies on the use of a low viscosity gold nanoparticle solution. Because of the low viscosity, the pressure required to get very high quality results is low enough to be compatible with the PDMS. Also, due to their size, gold nanoparticles have a significantly lower melting point than solid gold (about 140°C as opposed to about 1060°C respectively), low enough to be compatible with elastic and flexible materials that could be used as substrates [25]. Another important component according to Park et al. is the PDMS mould, which on top of being easy to replicate, allows for the evaporation of the organic solvents during the process, is easy to demould and is not very sensitive to contaminants [25]. Using this process, Park et al. fabricated arbitrary structures down to the nanometre scale, with the thinnest feature being 75nm wide. This is illustrated in Fig.20 below.



*Figure 20: Examples of gold nanostructures obtained by Park et al. on a polyimide substrate. a) Metallic nanowires with full width at half maximum (FWHM) of 75nm. b) Nanodots with full width at half maximum of 80nm. c) and d) are arbitrary structures with (1) being 400nm, (2) being 100nm and (3) being 100 nm wide. Taken from [25].*

The electrical and structural liability of the nanopatterns was further tested under successive bending cycles [25]. As it is visible from Fig.21, being subject to 65000 identical bending cycles had little impact in the integrity of the structures. In fact, there was no detectable difference from SEM images of the structures and their resistivity was unchanged within uncertainties [25].



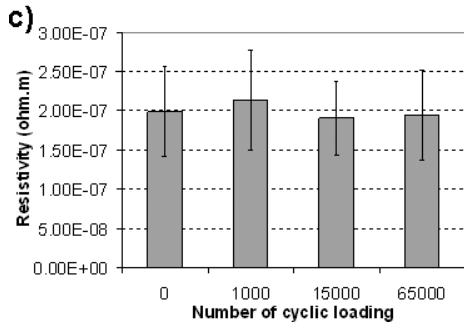


*Figure 21: a) Bending process setup. b) SEM images of the nanostructures before and after 65000 bending cycles. c) Electrical resistivity of the structures as a function of the number of bending cycles. Taken from [25].*

One drawback of this method is the fact that it does not allow for constant and controlled size of the structures in the vertical direction (see Fig.20 a) and b)). For instance, trapezoidal wires fabricated varied in height from 350nm to 420nm [25]. One needs to be aware of such a limitation if precise structures are needed in all 3 dimensions.

As it is visible from the presented papers, and in general, there is a lack of experimentation regarding SPP behaviour on bended and flexible surfaces, even though, in their theoretical approach, Pierre Berini and Junjie Lu [74] have demonstrated that long-range surface plasmons can exist in bended surfaces. It is desirable for further insight to be gained on the behaviour of surface plasmons over flexible surfaces, via suitable experimental and theoretical investigations.

Such insight could open many doors in exciting applications of bendable photonic circuits, especially with the recent advances in bendable electronics [11-21]. It is therefore interesting to end by reviewing some of the progress made in this area, which is closely related to the studied subject. The techniques used and presented below are also relevant in the broader context of the realisation of fully integrated, flexible, photo-electronic devices.

## **VI. Advances in flexible electronics**

In the subject, many comprehensive reviews have already been published [12,13,16,19], with the key points of the most recent one by Rogers et al. [12] presented here.

One branch of research in the field consists of using elastomers, such as PDMS, as a flexible substrate, and then placing on top of them conventional electronic materials in very thin form [12,14,19]. The elasticity, flexibility and deformability properties of the systems obtained are due to the shape and reduced thickness of the material [12,14]. Two successful configurations that were tested consist of either having a very thin 2D silicon in wavy forms on top of PDMS or having a 2D mesh that links to the PDMS only at the nodes [12]. These two configurations can be reversibly stretched, compressed, and

bended far beyond the limits of conventional silicon [12]. Another, slightly different in nature, occurrence of the use of mechanical configuration properties to achieve stretching properties can be seen in the work of Takao Someya et al. [17], which have fabricated a macroscopic net of pressure and thermal sensors. Organic transistors were used at the nodes of the net, and flexibility properties arose thanks to the macroscopic deformation of the shape of the net [17]. It is also interesting to note that somewhat complementary work has been carried out by Stephan C. B. Mannsfeld et al. [21], which have manufactured flexible pressure sensors with high performance and high sensitivity [21].

A different approach consists of using materials that inherently stretch rather than force the flexibility from the configuration [12]. One noticeable effort is made by Tsuyoshi Sekitani et al. [15], which have incorporated single-walled carbon nanotubes (SWNTs) [15, 75] as dopants in a fluorinated copolymer in order to obtain a flexible conductive material [12,15]. In order to further add elastic properties, this was also incorporated in a PDMS structure [12,15]. The resulting system was then limited by the elastic properties of the PDMS as opposed to the SWNTs [12]. The latter are erratically entangled within the flexible gel, and can reorganise themselves upon application of

stretching, in order to continue to allow for conductivity [12]. Using this material, Sekitani et al. [15] manufactured an active transistor matrix, and observed negligible change in performance under tensile stresses up to 70% [15], which demonstrates the effectiveness of the material.

## **VII. Discussion and Conclusions**

As it has been visible throughout this letter, an ideal, highly efficient, angle independent and broadband coupling method that is compatible with flexible substrates in compact systems has yet to be found. Different techniques allow for some of these objectives to be achieved, but this comes usually in detriment of other practical aspects. Prism coupling, with the most representative Kretschmann and Otto configurations [34,35,37], has the advantage of being generally quite simple and easy to use, both conceptually and practically, but relies on extended and rigid systems. More sophisticated methods using prisms can achieve miniaturisation (Kan et al. [51]), or somewhat broader coupling (O'Hara et al. [50]), but still do not display potential for integration in flexible systems. Optical fibbers have also been used as coupling devices, functioning in a way analogous to prisms, which can achieve better spatial confinement but are quite restrictive in that each fiber

must be maintained at a fixed angle with the plasmonic surface [59]. For better integration within electronic circuits, the plasmonic waveguide [62] and end-firing coupling [63] methods can be used, even though further improvement of these schemes is needed in order to make them compatible with a flexible environment. Finally, the most promising approach for broadband flexible plasmonics currently consists in using metamaterials [22-24]. Broadband coupling and fabrication of these surfaces on flexible substrates has already been achieved [22-24]. These methods rely however on sophisticated nanofabrication techniques [22-24], and it also seems that bending or stretching such surfaces would alter the properties of SPPs, even though more experimentation is needed in the area [22].

In this review, the fundamental aspects and theory behind plasmonics have been first addressed. The key issue of the field concerned with the excitation of surface plasmon polaritons that originates from a fundamental momentum mismatch between incident light and surface plasmon excitations due to their respective dispersion relations has been presented. Following this, the most important coupling methods have been reviewed, starting with the pioneering works of Kretschmann and Otto and ending with grating coupling and coupling through

metamaterials that are subject of increasing focus, in particular as they seem to display potential towards the realisation of plasmonics in flexible substrates. Finally, important advances in the field of flexible electronics have also been presented, which illustrate the potential of the field and motivate the interest in the realisation of elastic photonic devices. As it has been seen in this review, advances are significant and new methods and techniques continuously appear. However, there is still the need for further experimentation and characterisation of truly flexible plasmonic systems that display essential characteristics such as miniaturisation potential, broadband coupling and high efficiency before their integration into practical systems.

## References

- [1] UCD Plasmonics, Plasmonics and Ultrafast NanoOptics. n.d. *Surface Plasmons- a Brief History, Adapted from the Phd Thesis of Brian Ashall..* [online] Available at: [http://www.ucd.ie/biophysics/sp\\_history.html](http://www.ucd.ie/biophysics/sp_history.html) [Accessed: 6 Jan 2014].
- [2] Barnes, W. L., Dereux, A. and Ebbesen, T. W. 2003. Surface plasmon subwavelength optics. *Nature*, 424 pp. 824-830.
- [3] Zhang, J., Zhang, L. and Xu, W. 2012. Surface plasmon polaritons: physics and

- applications. *Journal of Physics D: Applied Physics*, 45 (11), p. 113001.
- [4] Zayats, A. V., Smolyaninov, I. I. and Maradudin, A. A. 2005. Nano-optics of surface plasmon polaritons. *Physics reports*, 408 (3), pp. 131--314.
- [5] Nicolas BONOD, Surface Plasmons: fundamentals and applications for photovoltaic cells, FrontNanoSpinPhoto conference presentation, available at: <http://www.cinam.univ-mrs.fr/confs/FrontNanoSpinPhoto/PDF/BOND.pdf> (November 17-19, 2009).
- [6] Maier, S. A., Brongersma, M. L., Kik, P. G., Meltzer, S., Requicha, A. A. and Atwater, H. A. 2001. Plasmonics\DNA Route to Nanoscale Optical Devices\*. *Adv. Mater*, 13 (19), p. 2.
- [7] Daghestani, H. N. and Day, B. W. 2010. Theory and applications of surface plasmon resonance, resonant mirror, resonant waveguide grating, and dual polarization interferometry biosensors. *Sensors*, 10 (11), pp. 9630--9646.
- [8] Ozbay, E. 2006. Plasmonics: merging photonics and electronics at nanoscale dimensions. *Science*, 311 (5758), pp. 189--193.
- [9] Hess, O., Pendry, J., Maier, S., Oulton, R., Hamm, J. and Tsakmakidis, K. 2012. Active nanoplasmonic metamaterials. *Nature materials*, 11 (7), pp. 573--584.
- [10] Homola, J., Yee, S. S. and Gauglitz, G. 1999. Surface plasmon resonance sensors: review. *Sensors and Actuators B: Chemical*, 54 (1-2), pp. 3-15.
- [11] Kim, D., Kim, Y., Wu, J., Liu, Z., Song, J., Kim, H., Huang, Y. Y., Hwang, K. and Rogers, J. A. 2009. Ultrathin Silicon Circuits With Strain-Isolation Layers and Mesh Layouts for High-Performance Electronics on Fabric, Vinyl, Leather, and Paper. *Advanced Materials*, 21 (36), pp. 3703--3707.
- [12] Rogers, J. A., Someya, T. and Huang, Y. 2010. Materials and mechanics for stretchable electronics. *Science*, 327 (5973), pp. 1603--1607.
- [13] Sun, Y. and Rogers, J. A. 2007. Inorganic semiconductors for flexible electronics. *Advanced Materials*, 19 (15), pp. 1897--1916.
- [14] Sun, Y., Choi, W. M., Jiang, H., Huang, Y. Y. and Rogers, J. A. 2006. Controlled buckling of semiconductor nanoribbons for stretchable electronics. *Nature nanotechnology*, 1 (3), pp. 201--207.
- [15] Sekitani, T., Noguchi, Y., Hata, K., Fukushima, T., Aida, T. and Someya, T. 2008. A rubberlike stretchable active matrix using elastic conductors. *Science*, 321 (5895), pp. 1468--1472.
- [16] Sekitani, T., Zschieschang, U., Klauk, H. and Someya, T. 2010. Flexible organic transistors and circuits with extreme bending stability. *Nature materials*, 9 (12), pp. 1015--1022.
- [17] Someya, T., Kato, Y., Sekitani, T., Iba, S., Noguchi, Y., Murase, Y., Kawaguchi, H. and

- Sakurai, T. 2005. Conformable, flexible, large-area networks of pressure and thermal sensors with organic transistor active matrixes. *Proceedings of the National Academy of Sciences of the United States of America*, 102 (35), pp. 12321--12325.
- [18] Ko, H. C., Shin, G., Wang, S., Stoykovich, M. P., Lee, J. W., Kim, D., Ha, J. S., Huang, Y., Hwang, K. and Rogers, J. A. 2009. Curvilinear electronics formed using silicon membrane circuits and elastomeric transfer elements. *Small*, 5 (23), pp. 2703--2709.
- [19] Sekitani, T. and Someya, T. 2010. Stretchable, Large-area Organic Electronics. *Advanced Materials*, 22 (20), pp. 2228--2246.
- [20] Klauk, H., Halik, M., Zschieschang, U., Eder, F., Rohde, D., Schmid, G. and Dehm, C. 2005. Flexible organic complementary circuits. *Electron Devices, IEEE Transactions on*, 52 (4), pp. 618--622.
- [21] Mannsfeld, S. C., Tee, B. C., Stoltenberg, R., Chen, C. V. H., Barman, S., Muir, B. V., Sokolov, A. N., Reese, C. and Bao, Z. 2010. Highly sensitive flexible pressure sensors with microstructured rubber dielectric layers. *Nature materials*, 9 (10), pp. 859--864.
- [22] Aksu, S., Huang, M., Artar, A., Yanik, A. A., Selvarasah, S., Dokmeci, M. R. and Altug, H. 2011. Flexible plasmonics on unconventional and nonplanar substrates. *Advanced Materials*, 23 (38), pp. 4422--4430.
- [23] Sun, S., He, Q., Xiao, S., Xu, Q., Li, X. and Zhou, L. 2012. Gradient-index meta-surfaces as a bridge linking propagating waves and surface waves. *Nature materials*, 11 (5), pp. 426--431.
- [24] Di Falco, A., Ploschner, M. and Krauss, T. F. 2010. Flexible metamaterials at visible wavelengths. *New Journal of Physics*, 12 (11), p. 113006.
- [25] Park, I., Ko, S. H., Pan, H., Grigoropoulos, C. P., Pisano, A. P., Fr'echet, J. M., Lee, E. and Jeong, J. 2008. Nanoscale patterning and electronics on flexible substrate by direct nanoimprinting of metallic nanoparticles. *Advanced Materials*, 20 (3), pp. 489--496.
- [26] Humboldt-Universitat zu Berlin, Olivier Benson, Chapter 7: Plasmonics, available through <http://www.physik.hu-berlin.de/nano/lehre/Gastvorlesung%20Wien/> or directly at <http://www.physik.hu-berlin.de/nano/lehre/Gastvorlesung%20Wien/plasmonics> [visited 6 January 2014].
- [27] Pitarke, J., Silkin, V., Chulkov, E. and Echenique, P. 2007. Theory of surface plasmons and surface-plasmon polaritons. *Reports on progress in physics*, 70 (1), p. 1.
- [28] Freestone, I., Meeks, N., Sax, M. and Higgitt, C. 2007. The Lycurgus cup—a roman nanotechnology. *Gold Bulletin*, 40 (4), pp. 270--277.
- [29] Wood, R. W. 1902. On a Remarkable Case of Uneven Distribution of Light in a Diffraction Grating Spectrum. *Proceedings of the Physical Society of London*, 18 (1), p. 269.

- [30] Wood, R. 1912. XXVII. Diffraction gratings with controlled groove form and abnormal distribution of intensity. *Philosophical Magazine Series 6*, 23 (134), pp. 310-317.
- [31] Stern, E. A. and Ferrell, R. A. 1960. Surface Plasma Oscillations of a Degenerate Electron Gas. *Phys. Rev.*, 120 pp. 130-136.
- [32] Ritchie, R., Arakawa, E., Cowan, J. and Hamm, R. 1968. Surface-plasmon resonance effect in grating diffraction. *Physical Review Letters*, 21 (22), p. 1530.
- [33] Mcphedran, R. and Maystre, D. 1974. A detailed theoretical study of the anomalies of a sinusoidal diffraction grating. *Journal of Modern Optics*, 21 (5), pp. 413--421.
- [34] Otto, A. 1968. Excitation of nonradiative surface plasma waves in silver by the method of frustrated total reflection. *Zeitschrift für Physik*, 216 (4), pp. 398--410.
- [35] Kretschmann, E. and Reather, H. 1968. Radiative decay of nonradiative surface plasmon excited by light. *Z. Naturf.*, 23A p. 2135.
- [37] Maier, S. A. 2007. *Plasmonics: Fundamentals and Applications*. [New York]: Springer Science+Business Media, LLC.pp.5-52
- [38] Enoch, S. and Bonod, N. 2012. *Plasmonics*. Heidelberg [etc.]: Springer. pp.269-285.
- [39] Pease, R. 1981. Electron beam lithography. *Contemporary Physics*, 22 (3), pp. 265--290.
- [40] Maier, S. A. 2007. *Plasmonics: Fundamentals and Applications*. [New York]: Springer Science+Business Media, LLC.pp.159-170.
- [41] Utke, I., Hoffmann, P. and Melngailis, J. 2008. Gas-assisted focused electron beam and ion beam processing and fabrication. *Journal of Vacuum Science \& Technology B: Microelectronics and Nanometer Structures*, 26 (4), pp. 1197--1276.
- [42] Spin Coat Theory, Spin Coating Process theory, e e Cost Effective Equipment, available at:  
<http://www.clean.cise.columbia.edu/process/spintheory.pdf> [visited 7 January 2014]
- [43] Norrman, K., Ghanbari-Siahkali, A. and Larsen, N. 2005. 6 Studies of spin-coated polymer films. *Annual Reports Section C"(Physical Chemistry)*, 101 pp. 174--201.
- [44] Jackson, J. D. 1999. *Classical electrodynamics*. 3<sup>rd</sup> ed. New York: Wiley.
- [45] Marder, M. P. 2010. *Condensed matter physics*. 2<sup>nd</sup> ed. Hoboken, N.J.: Wiley.
- [46] Bora Ung, 5 Surface plasmon polaritons: theoretical framework, *Collection Mémoires et thèses électroniques*, Université Laval, 2007, available at :  
<http://theses.ulaval.ca/archimede/fichiers/24879/ch05.html> [visited January 8 2014]
- [47] Griffiths, D. J. 1999. *Introduction to electrodynamics*. Upper Saddle River, N.J.: Prentice Hall.

- [48] ScottTParker, File: Prism Coupler.png, *Wikipedia, The Free Encyclopedia*, 4 Dec. 2007, available at [http://en.wikipedia.org/wiki/File:Prism\\_Coupler.png](http://en.wikipedia.org/wiki/File:Prism_Coupler.png) [visited 4 January 2014].
- [49] Wang, H. 1995. Coupling to surface plasmon waves by the use of a birefringent prism coupler. *Optics communications*, 119 (1), pp. 75--77.
- [50] O'hara, J., Averitt, R. and Taylor, A. 2005. Prism coupling to terahertz surface plasmon polaritons. *Optics express*, 13 (16), pp. 6117--6126.
- [51] Kan, T., Tsujiuchi, N., Iwase, E., Matsumoto, K. and Shimoyama, I. 2010. Planar near-infrared surface plasmon resonance sensor with Si prism and grating coupler. *Sensors and Actuators B: Chemical*, 144 (1), pp. 295--300.
- [52] Hurtado-Ramos, J. and Wang, H. 1997. Analysis of accuracy in prism coupling methods and a proposal of two simple ways for coupling to guided waves and/or for exciting surface plasmon resonance. *Optical Materials*, 7 (4), pp. 153--164.
- [53] Sherry, L. J., Jin, R., Mirkin, C. A., Schatz, G. C. and Van Duyne, R. P. 2006. Localized surface plasmon resonance spectroscopy of single silver triangular nanoprisms. *Nano letters*, 6 (9), pp. 2060--2065.
- [54] Chen, W., Ritchie, G. and Burstein, E. 1976. Excitation of surface electromagnetic waves in attenuated total-reflection prism configurations. *Physical review letters*, 37 (15), p. 993.
- [55] Charbonneau, R. and Berini, P. 2008. Broadside coupling to long-range surface plasmons in metal stripes using prisms, particles, and an atomic force microscope probe. *Review of Scientific Instruments*, 79 (7), pp. 073106--073106.
- [56] Jin, R., Cao, Y., Mirkin, C. A., Kelly, K., Schatz, G. C. and Zheng, J. 2001. Photoinduced conversion of silver nanospheres to nanoprisms. *Science*, 294 (5548), pp. 1901--1903.
- [57] Li, W., Ma, H., Zhang, J., Liu, X. and Feng, X. 2009. Fabrication of gold nanoprism thin films and their applications in designing high activity electrocatalysts. *The Journal of Physical Chemistry C*, 113 (5), pp. 1738--1745.
- [58] Pastoriza-Santos, I. and Liz-Marzá'n, L. M. 2002. Synthesis of silver nanoprisms in DMF. *Nano Letters*, 2 (8), pp. 903--905.
- [59] Charbonneau, R., Lisicka-Shrzek, E. and Berini, P. 2008. Broadside coupling to long-range surface plasmons using an angle-cleaved optical fiber. *Applied Physics Letters*, 92 (10), pp. 101102--101102.
- [60] Hecht, B., Bielefeldt, H., Novotny, L., Inouye, Y. and Pohl, D. 1996. Local excitation, scattering, and interference of surface plasmons. *Physical Review Letters*, 77 (9), p. 1889.
- [61] Bouhelier, A. and Wiederrecht, G. 2005. Excitation of broadband surface plasmon

- polaritons: Plasmonic continuum spectroscopy. *Physical Review B*, 71 (19), p. 195406.
- [62] Tian, J., Yu, S., Yan, W. and Qiu, M. 2009. Broadband high-efficiency surface-plasmon-polariton coupler with silicon-metal interface. *Applied Physics Letters*, 95 (1), pp. 013504--013504.
- [63] Stegeman, G., Wallis, R. and Maradudin, A. 1983. Excitation of surface polaritons by end-fire coupling. *Optics letters*, 8 (7), pp. 386-388.
- [64] Hooper, I. R. and Sambles, J. R. 2003. Surface plasmon polaritons on thin-slab metal gratings. *Physical Review B*, 67 (23), p. 235404.
- [65] Cesario, J., Quidant, R., Badenes, G. and Enoch, S. 2005. Electromagnetic coupling between a metal nanoparticle grating and a metallic surface. *Optics letters*, 30 (24), pp. 3404--3406.
- [66] Yoon, J., Song, S. H. and Kim, J. 2008. Extraction efficiency of highly confined surface plasmon-polaritons to far-field radiation: an upper limit. *Optics express*, 16 (2), pp. 1269--1279.
- [67] Lin, L., Blaikie, R. and Reeves, R. 2005. Surface-plasmon-enhanced optical transmission through planar metal films. *Journal of Electromagnetic Waves and Applications*, 19 (13), pp. 1721--1728.
- [68] Chen, C. and Berini, P. 2010. Grating couplers for broadside input and output coupling of long-range surface plasmons. *Optics Express*, 18 (8), pp. 8006--8018.
- [69] Offerhaus, H., Van Den Bergen, B., Escalante, M., Segerink, F., Korterik, J. and Van Hulst, N. 2005. Creating focused plasmons by noncollinear phasematching on functional gratings. *Nano letters*, 5 (11), pp. 2144--2148.
- [70] Ropers, C., Neacsu, C., Elsaesser, T., Albrecht, M., Raschke, M. and Lienau, C. 2007. Grating-coupling of surface plasmons onto metallic tips: a nanoconfined light source. *Nano letters*, 7 (9), pp. 2784--2788.
- [71] Devaux, E., Ebbesen, T. W., Weeber, J. and Dereux, A. 2003. Launching and decoupling surface plasmons via micro-gratings. *Applied physics letters*, 83 (24), pp. 4936--4938.
- [72] Miccio, L., Paturzo, M., Finizio, A. and Ferraro, P. 2010. Light induced patterning of poly (dimethylsiloxane) microstructures. *Optics express*, 18 (11), pp. 10947--10955.
- [73] Smart Lighting. 2012. *Sensors Research Thrust Strategic Goals*. [online] Available at: <http://smartlighting.rpi.edu/research/sensor.s.shtml> [Accessed: 8 Jan 2014].
- [74] Berini, P. and Lu, J. 2006. Curved long-range surface plasmon-polariton waveguides. *Optics Express*, 14 (6), pp. 2365--2371.
- [75] Cao, Q. and Rogers, J. A. 2009. Ultrathin Films of Single-Walled Carbon Nanotubes for Electronics and Sensors: A Review of Fundamental and Applied Aspects. *Advanced Materials*, 21 (1), pp. 29--53.
- [76] Feng, N. and Dal Negro, L. 2007. Plasmon

mode transformation in modulated-index metal-dielectric slot waveguides. *Optics letters*, 32 (21), pp. 3086--3088.

[77] Feng, N., Brongersma, M. L. and Negro, L. 2007. Metal-Dielectric Slot-Waveguide

Structures for the Propagation of Surface Plasmon Polaritons at 1.55  $\mu$ m. *Quantum Electronics, IEEE Journal of*, 43 (6), pp. 479--485.